

Research Article

Grid-Connected Semitransparent Building-Integrated Photovoltaic System: The Comprehensive Case Study of the 120kWp Plant in Kunming, China

Yunfeng Wang ¹, Ming Li ¹, Reda Hassanien Emam Hassanien,^{1,2} Xun Ma ¹,
and Guoliang Li¹

¹Solar Energy Research Institute, Yunnan Normal University, Kunming, China

²Agricultural Engineering Department, Cairo University, Giza 12613, Egypt

Correspondence should be addressed to Xun Ma; maxun80313@126.com

Received 11 September 2017; Accepted 14 December 2017; Published 13 March 2018

Academic Editor: Gabriele Battista

Copyright © 2018 Yunfeng Wang et al. This is an open access article distributed under the Creative Commons Attribution License, which permits unrestricted use, distribution, and reproduction in any medium, provided the original work is properly cited.

A 120 kWp building-integrated photovoltaic (BIPV) system was installed on the south facade of the Solar Energy Research Institute building in Yunnan Normal University. The area of the curtain wall was 1560 m² (26 m × 60 m), which consisted of 720 semitransparent monocrystalline silicon double-glazing PV panels. This paper studied the yearly and monthly variations of power generation in terms of solar data and meteorological parameters. The total amount of power generation of the BIPV system measured from October 2014 to September 2015 was 64.607 MWh, and the simulation results with TRNSYS (Transient Systems Simulation Program) provided the 75.515 MWh predicted value of annual electricity production with the meteorological database of Meteonorm, while, based on the average value of the performance ratio (PR) of 60% and the life cycle assessment (LCA) of the system, the energy payback time (EPBT) of 9.38 years and the potential for pollutant emission reductions have been evaluated and the environmental cost is RMB ¥0.01053 per kWh. Finally, an economic analysis was carried out; the net present value (NPV) and the economic payback time of the BIPV system were estimated to be RMB ¥359,347 and 15 years, respectively.

1. Introduction

In the last 20 years, the world's energy consumption has sharply increased (40%), and it is expected to continue increasing by one-third in the period 2035 [1]. 20% to 40% of this global energy is consumed in the built environment [2]. In China, building energy consumption has been continuously increasing, which has been doubled during the last decades in China [3]. According to the growing trend of developed countries, the building energy consumption will account for at least 40% of all social total energy consumption in China [4]. In this situation, (nearly) zero-energy buildings (NZEB) have been considered the priority solutions for the architecture trend in the future. NZEB implies that all building-related operating energy is generated on the building site itself by renewable sources [5]. One of the most promising approaches to realize NZEB is by adopting

solar energy-generating devices in the form of photovoltaic (PV) modules for electricity. As a kind of new energy, solar energy is the most abundant and inexhaustible, so several policies have been proposed by the Chinese government, such as the plan of the solar roof of buildings [6]. However, in modern urban cities, most buildings are high-rise and the roof area would be very limited for stand-alone PV system installation [7]. So the integration of PV systems into buildings becomes an imperative [8]. Building-integrated photovoltaics (BIPV) replacing part of the external walls with PV panels would be an appropriate alternative form of the PV system [9]. Integration of PV systems with distribution networks (grid-connected) could reduce the maximum demand charge and energy losses [10]. Moreover, BIPV can serve as a shading device for a window, a semitransparent glass facade, a building exterior cladding panel, a skylight, and a parapet unit or roofing system [11].

Li et al. [12] investigated the energy performance of a semitransparent a-Si PV facade. The simulation results revealed that the semitransparent PV facade was able to reduce the annual building energy use and peak cooling load by 1203 MWh and 450 kW, respectively. And in 2013, they conducted a study of the operational performance of a grid-connected BIPV system in Hong Kong. Annually, the electricity generation of 42,450 kWh was recorded and emissions of CO₂, SO₂, NO_x, and particulates could be reduced, respectively, by 32 tons, 43.3 kg, 41.8 kg, and 2.07 kg [13]. Furthermore, Hong et al. conducted a sensitivity analysis on how the impact factors of the rooftop PV system affect its electricity generation and developed a GIS-based optimization model for estimating the electricity generation of the rooftop PV system [14]. On a fixed PV array performance, its best electrical configuration had been researched by analyzing annual energy production with the surrounding obstacles causing partial shading conditions [15]. And the multiple calculations had been provided to determine whether solar energy has a viable strategic role in the global energy market [16]. The embodied energy payback period for a photovoltaic system integrated with the building was reported within the range of 12–13 years for the southern and western facades in the United Arab Emirates [17]. Besides, a lot of the previous studies researched the energy harvested and evaluated the performance of BIPV systems [18–21].

However, there is still a lack of research on the performance of semitransparent BIPV facades compared with conventional glazing in low-latitude and high-altitude cities, such as the city of Kunming. This experiment was the first and largest BIPV application installed on the building facade of the Solar Energy Research Institute of Yunnan Normal University. Thus, the aim of this paper is to analyze the PV power generation performance and evaluate the economic benefits of a grid-connected semitransparent BIPV system. The energy output and meteorological data were recorded and analyzed, and a TRNSYS (Transient Systems Simulation Program) model was built; the net energy benefit, carbon emission reduction, and cost savings as well as energy, carbon emissions, and cost payback were evaluated by using life cycle assessment (LCA). The results can be used to evaluate the performance and provide the reference data for more applications of semitransparent BIPV under the actual operating environments.

2. BIPV System Description

The BIPV system was built in Kunming City in June 2014; then, it was put into operation in October 2014. Kunming City at the southwest of China is a special plateau city, which receives an annual total solar radiation at the horizontal plane of $\sim 1530.24 \text{ kWh/m}^2$. It also has the mildest climates characterized by short, cool dry winters with mild days and crisp night, and long, warm, and humid summers. Therefore, the climate and location of Kunming are suitable for the development of solar energy, and a lot of PV systems have been built and running in Kunming. The first and largest grid-connected semitransparent BIPV system of Kunming in this study (Figure 1) was installed outside of



FIGURE 1: Yunnan Normal University BIPV system.

the south facade of the building of the Solar Energy Research Institute in Yunnan Normal University. The BIPV system was 60 m in length and 26 m in height at the south face of the 5-storey building with a total area of 1560 m², including 720 monocrystalline silicon double-glazing PV modules. The modules were installed with 85° tilt angles and were 6 m apart from the building for the ventilation. The PV arrays were comprised of 30 parallel strings where each string has 24 modules, and the peak power and voltage of each string were 4080 Wp and 796 V, respectively. The specifications of the semitransparent PV modules are given in Table 1. Each PV module with dimensions of 1985 × 1038 mm consisted of 64 pieces of the solar cell and a 6 mm transparent glass cover, a 6 mm glass backside, and a certain space between the PV cells to transmit light in order to ensure a 47% light transmittance as shown in Figure 2. Solar cells adopted in the PV module were monocrystalline silicon wafer cells with an 8.25% efficiency, and the dimensions of each cell were 125 × 125 mm. The reason why the efficiency of the PV module was lower than that of the conventional monocrystalline silicon module was that the areas of the 64 pieces of solar cells in a module were just 48.5% of the total area of a PV module. It was based on the cost of sacrificing the efficiency of the PV module to ensure partial light transmission. The laminated glass forms were installed on both the west and east directions and on the rooftops of the PV curtain wall (Figure 3). And some ventilation blinds were placed at the top and the bottom of the PV curtain wall for proper ventilation (Figure 4). The PV module temperature will be controlled or affected according to the adjustment of these ventilation blinds by opening or closing it in different seasons.

The 720 solar modules were configured to 25 (parallel) × 24 (series) and 5 (parallel) × 24 (series). The 600 modules were connected to the inverter (Growatt CP100 with a matching maximum DC voltage of 1000 V and a maximum input current of 250 A, maximum efficiency of 97.1%, and maximum DC input power of 115 kW), and the remaining 120 modules were connected to another inverter (Growatt 20000UE with a matching maximum DC voltage of 1000 V and a maximum input current of 20 A, maximum efficiency of 98%, and maximum DC input power of 20.8 kW). The 120 kWp power generated was synchronized and supplied

TABLE 1: The PV module specifications under standard test conditions (STCs).

Number	Item	Parameter
1	Dimensions of one module (mm)	1985 × 1038 × 13.52
2	Weight of one module (kg)	63
3	Light transmittance	47%
4	Nominal power of one module (Wp)	170
5	Short-circuit current (A)	5.65
6	Open-circuit voltage (V)	39.6
7	Efficiency	8.25%
8	Maximum power point current (A)	5.12
9	Maximum power point voltage (V)	33.2
10	Layer structure	Toughened glass (6 mm) + PVB (2.28 mm) + (125 × 125 mm) sc-Si cells + toughened glass (6 mm)

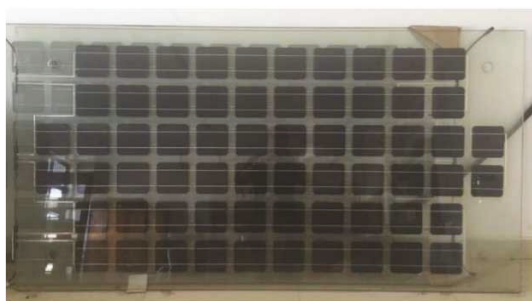


FIGURE 2: The semitransparent double-glazing PV module.



FIGURE 3: The inside view of the PV curtain wall.

to the 400 V campus grid through a grid export conditioner. The Maximum Power Point Tracker (MPPT) was used to adjust the voltage of the PV generator to operate at its maximum power point.

Figure 5 shows the schematic diagram of the electrical system and the monitoring system, and each data is collected by 2 photovoltaic inverters connected with a power-monitoring module bus to investigate the generating characteristics of the BIPV system. A pyrhelimeter, thermometers, a watt-hour meter, and so forth are also installed to collect the data needed for a detailed analysis of the BIPV system.

3. BIPV System Performance Analysis

3.1. Experimental Analysis of Power-Generating Performance of BIPV. Figure 6 shows the amount of power generation in the building from October 2014 to September 2015 monthly. The monthly average amount of generation was 5383.9 kWh, while the cumulative amount for 12 months was 64,607.5 kWh. The month with the least generated amount (740.2 kWh) was September. This is because of the installation tilt and operating temperature. The BIPV system was installed with an 85° tilt angle facing towards the south, due to the solar zenith angle being high in summer, so that the solar irradiation received by the PV modules decreased significantly in September. Besides, the generated amount (1664.9 kWh) was also less in March. This is because February and March in Kunming's climate correspond to the coldest season. This was especially true, and it even snowed in 2015, so the solar radiation sharply lowered with the extended severe climate and affected the power generation; however, this kind of extreme weather was just for the year 2015. The month with the highest generated amount (11,025 kWh) was December, up to 14.9 times compared with that in September.

However, the operating temperature (or the panel temperature) of PV modules seems to be a little different between summer and winter for Kunming City, as shown in Figure 7(a), which shows the average operating temperature of PV modules in the sunny days of June 14 and December 15. It was found that the average operating temperature of summer and winter before 8:29 in the morning was identical, while in the noon, the temperature in winter was about 10°C higher than the operating temperature of summer. The operating temperatures of both days increased rapidly from 9:00, and about 3 hours later, the temperatures reached the maximum temperature and then gradually decreased and got close to each other. One of the reasons why the average operating temperature was lower in summer was that the ventilation blinds on the top and bottom of the PV curtain wall as shown in Figure 4 were opened in order to decrease the air temperatures and reduce the cooling load of the building. Although the operating temperature of the PV module in December was up to



FIGURE 4: The ventilation blinds at the top and bottom of the PV curtain wall.

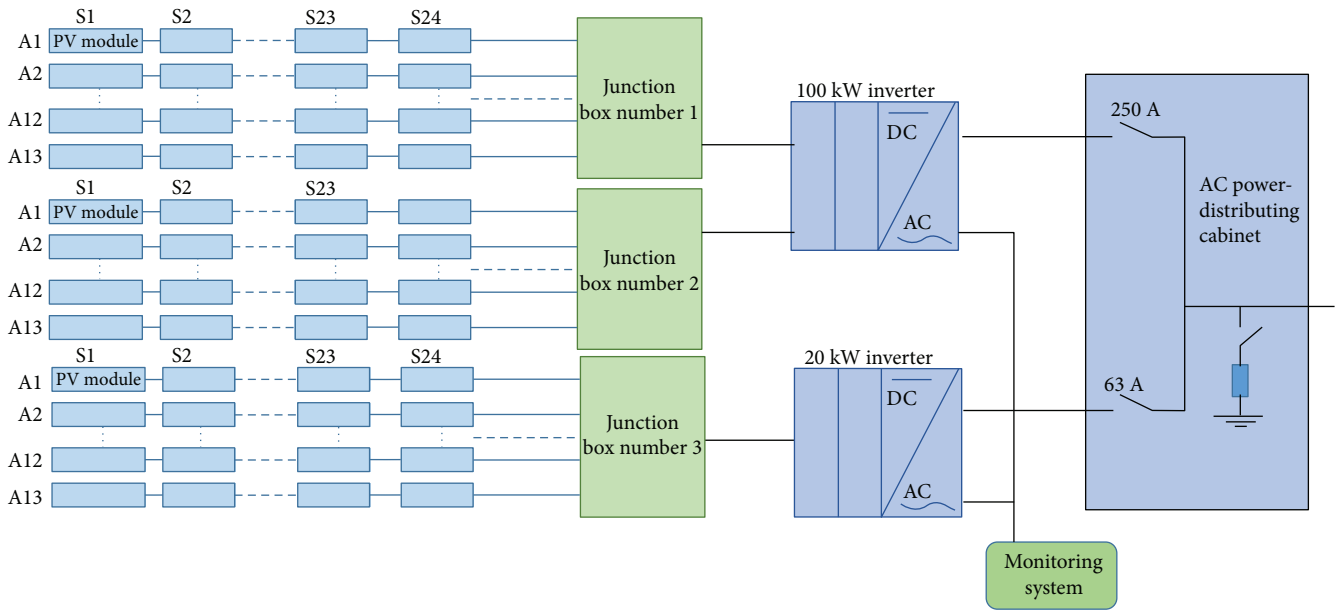


FIGURE 5: The connection schematic diagram of the system.

55.2°C, the air temperature in the gap between the PV curtain wall and the exterior wall of the building was just 32°C, and the average of the 1st–5th floor temperatures eventually reached around 22°C, which was 6°C higher than the ambient temperature as shown in Figure 7(b). Because the ventilation blinds on the top and bottom of the PV curtain wall were closed, the increased air temperature could be used to keep the rooms warm without any auxiliary heating in winter. Another reason was that the PV modules can receive more solar irradiation in winter because of the installed inclination angles of the PV curtain wall. The solar radiation intensity on the surface of the PV curtain facing south with an 85° tilt angle in the two typical sunny days of June 2015 and December 2014 is shown in Figure 8. The highest and average solar radiation intensities on the vertical surface of the PV modules (957 W/m² and 417 W/m²) in a typical day of December were both up to 2 times higher than those in June (495 W/m² and 233 W/m²), respectively. It

seems that the solar radiation would have the largest effect on the power generation. Furthermore, the daily power generation in December of 2014 and in the two identical months of 2014 and 2015 is shown in Figures 9 and 10, respectively. It indicates that the daily power generation may fluctuate greatly even in the same month of different years, due to the solar radiation variation which was the typical climate in Kunming.

3.2. TRNSYS Simulation Results and Discussion. TRNSYS is a transient system energy modeling software developed to solve complex energy system problems. The software uses individual components referred to as types connected to each other with each representing one part of the overall system. Figure 11 shows the TRNSYS model used to simulate the power generation of the PV system, which has a weather database to predict the behavior of PV installations in many locations such as Kunming. In this work, a five-parameter

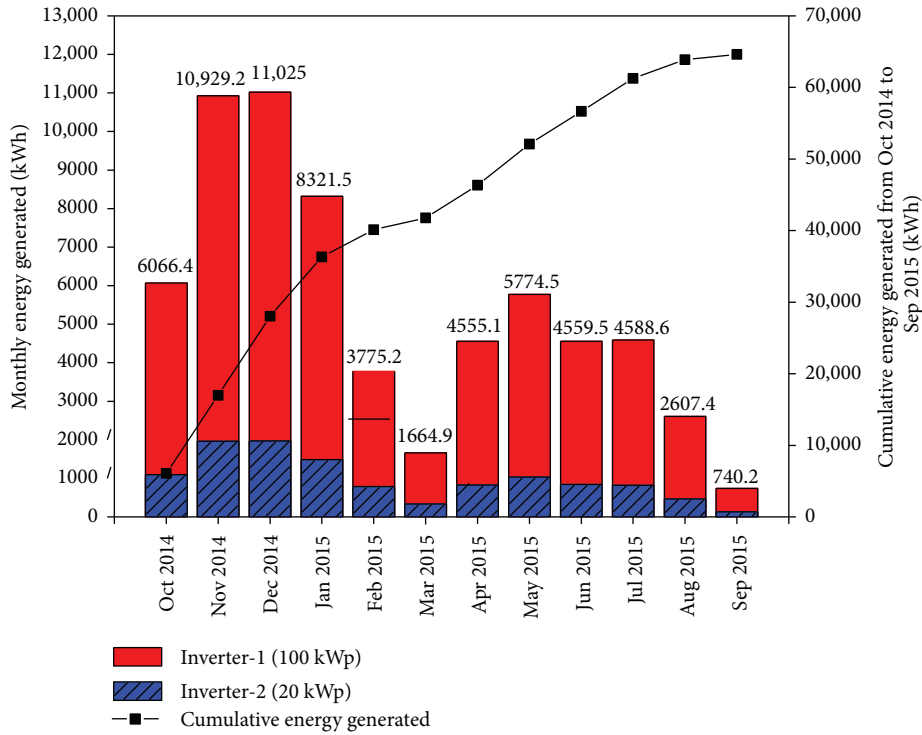


FIGURE 6: Amount of monthly power generation.

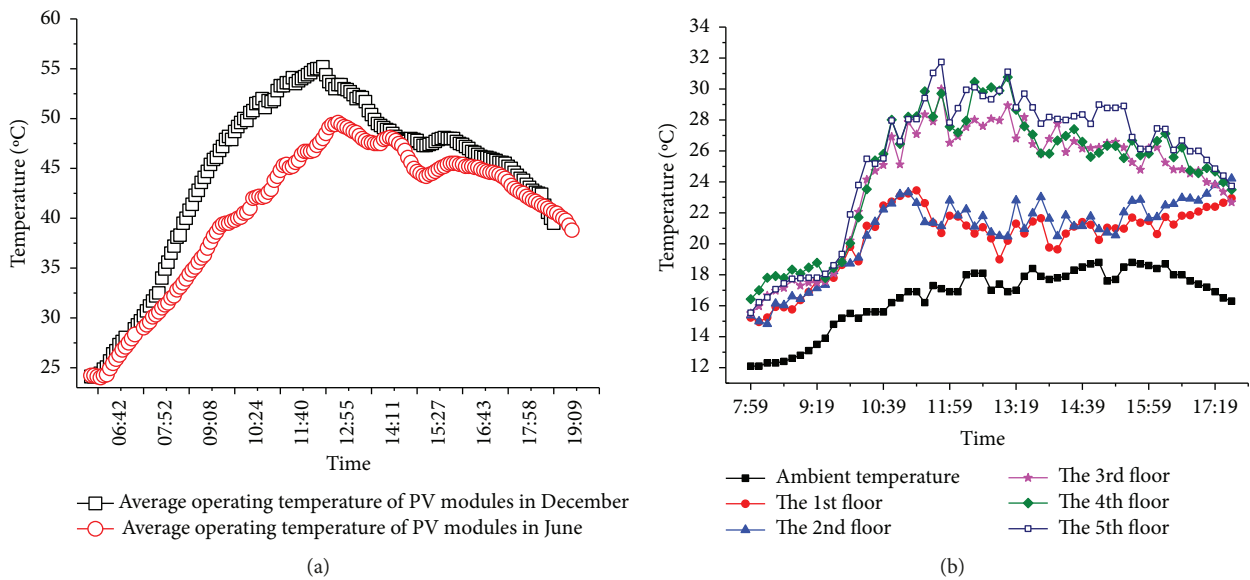


FIGURE 7: (a) The average operating temperature of PV modules and (b) the air temperature in the gap between the PV curtain wall and the exterior wall of the building.

model (Type 194 “photovoltaic array”) has been used to determine the maximum power point from $I-V$ curves in the operating conditions which are given by the meteorological inputs. The inverter information is given as a text file to the PV component in Type 194.

3.2.1. TRNSYS Model Validation. The PV system model was created using TRNSYS 16 with known photovoltaic cell

envelope characteristics. The model was then validated with the data collected using pyrheliometers, thermometers, and so forth. The meteorological inputs used in the Type 109-User were the in-field monitoring data. From the results of the data collection, a curve was developed illustrating the power output of one day with respect to the solar radiation. This curve was used to validate the TRNSYS model by matching the TRNSYS power outputs at various solar

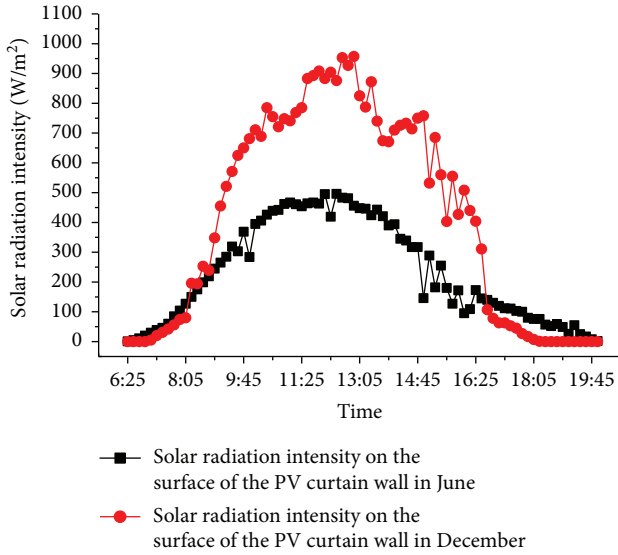


FIGURE 8: Solar radiation intensity on the vertical surface of the PV curtain wall.

radiations. Figure 12 demonstrates the power output of the 20 kW inverter array parts at a monitoring weather condition which was matched with the TRNSYS model power output. The weather condition and PV power output of the day of November 25, 2015, had been chosen to verify the accuracy of the TRNSYS model.

It could be found from Figure 12 that there were some differences between the hourly measured power output and the simulation results with the TRNSYS model on a sunny day. Maybe the reason was that the temperature provided to Type 194 was the ambient temperature during the test periods and not the real temperature of the PV curtain wall; in addition, the solar radiation intensity provided to Type 109 was the total radiation on the horizontal. Type 194 used temperature data from the standard NOCT (nominal operating cell temperature) measurements to compute the module temperature T_c at each time step. The NOCT temperature is the operating temperature of the module with a wind speed of 1 m/s, no electrical load, and a certainly specified insolation and ambient temperature. Besides, Type 194 uses the NOCT data to determine the ratio of the module transmittance-reflectance product to the module loss coefficient [22]. And indeed, the literature shows that the choice of the temperature model is relevant only on a daily basis but has a small effect on the annual predicted PV output [23]. Besides, the calculation of the radiation on a tilted surface derives from the radiation on the horizontal surface. This calculation involves the use of a global diffuse correlation and of a tilted surface radiation model to estimate the direct, diffuse, and albedo components of the radiation on the tilted surface. The literature has shown that the Perez model (model 4 in TRNSYS) can be a good choice to predict the energy output. However, the relative error of the hourly power generation was less than 17%, and the relative error of the average hourly power generation was just 6.25%. The calculated result agreed with the measured result on the

amount of power generation of the day, 98.6 kWh and 104.4 kWh, respectively, and the relative error between the measured result and simulation result was 5.55%. In general terms, the five-parameter model (Type 194) provides a simple tool to predict the PV production accurately.

3.2.2. The BIPV Energy Output according to the TRNSYS Model. The yearly energy PV production has been calculated with TRNSYS, using the meteorological database of Meteororm and Type 109 and assuming that the PV installation is connected to the grid with no failures. The annual PV power generation for the BIPV system is shown in Figure 13. The results reveal that the calculated annual electricity production of the BIPV is about 75.515 MWh. On the other hand, the monthly peak production was reached in November with 9.67 MWh and the lowest was found in June with 3.789 MWh.

4. Analysis and Discussion

4.1. Performance Assessment. In order to identify the performance of the BIPV system, the performance ratio (PR) was calculated. The PR, which is a crucial parameter for the PV performance evaluation, describes the relationship between the actual and theoretical energy outputs of the PV array. It represents the energy losses such as loss due to temperature, wiring loss, shadowing, soiling, inverter, mismatch loss, and loss across the bypass diodes and shows the incomplete utilization of incoming solar radiation and proportion of energy available at the grid after losses in grid-connected PV systems. It is the most widely used performance parameter for comparative analysis of different PV panel technologies and is also used for comparing grid-connected PV systems irrespective of their location, power capacity, and mounting structure [24]. The main equation was used to investigate the PR as follows [25]:

$$PR = \frac{E_{y-s}}{(H/1000) \times P_{n-s}}, \quad (1)$$

where E_{y-s} is the energy generated by the PV system during the year [Wh], H is the annual solar irradiation on the PV modules [Wh/m²·year], and P_{n-s} is the nominal power of the system measured at STC [Wp].

According to the test data of the first year of installation (the year 2015), the PR of the BIPV system is calculated as being equal to 64.3%, which includes some extreme weather events like snows in this year. The BIPV system has just run for two years since it was completed; more precise data for calculating the performance ratio of the system have not been acquired during its working period. However, such PR value can be considered within the normal range; literature showed that PV arrays installed in Italy have a PR value varying across the range from 62% to 81% [26], though it has a different tilt angle and different system structure. Some research shows that the climatic conditions have a great impact on the PR [27]. For example, the year that had the greatest number of days with bad weather (rain, snow, or fog) had the lower PR; on the contrary, the highest PR

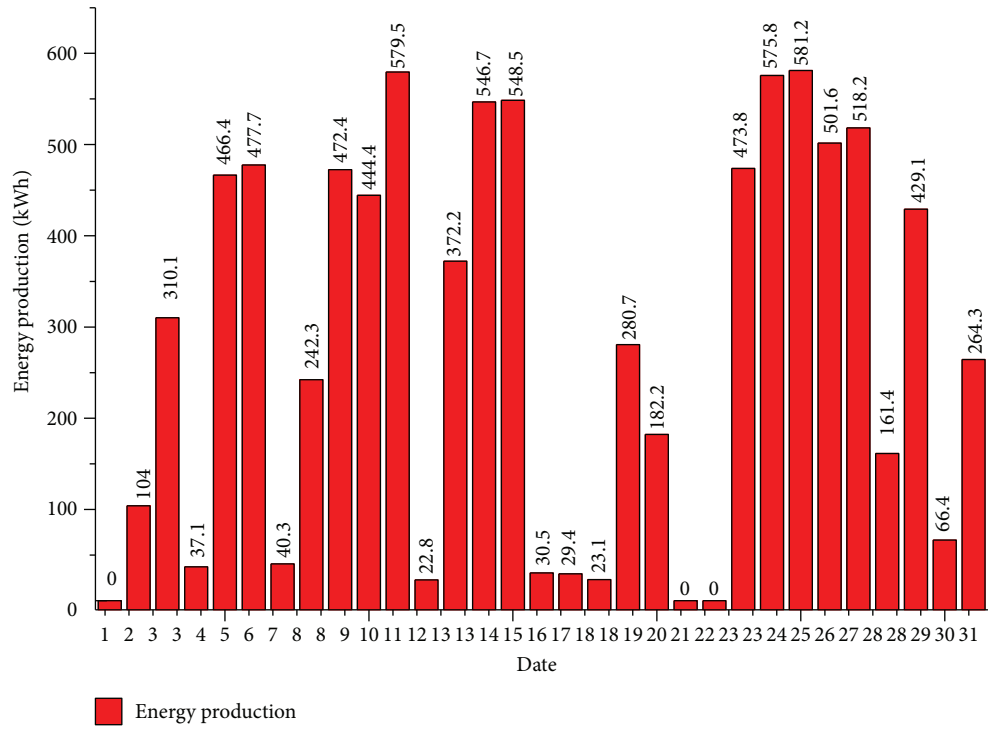


FIGURE 9: Daily December power generation.

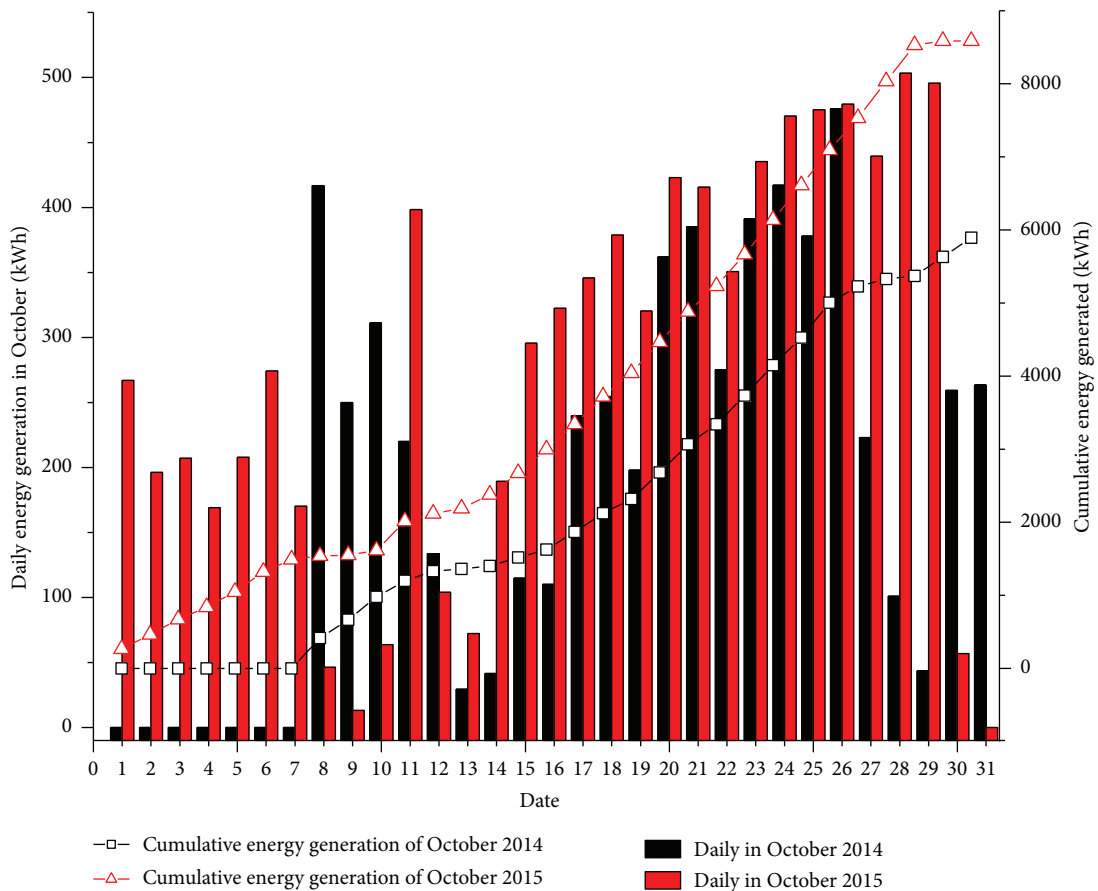


FIGURE 10: Power generation compared in the same month of different years.

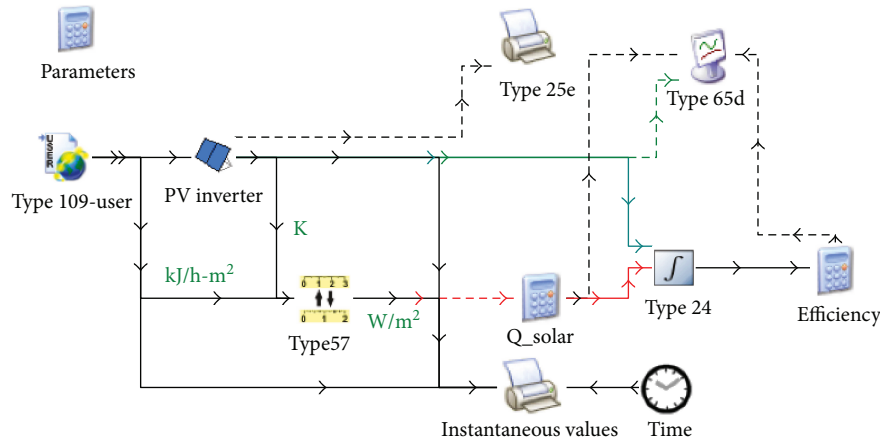


FIGURE 11: Scheme of the TRNSYS PV model.

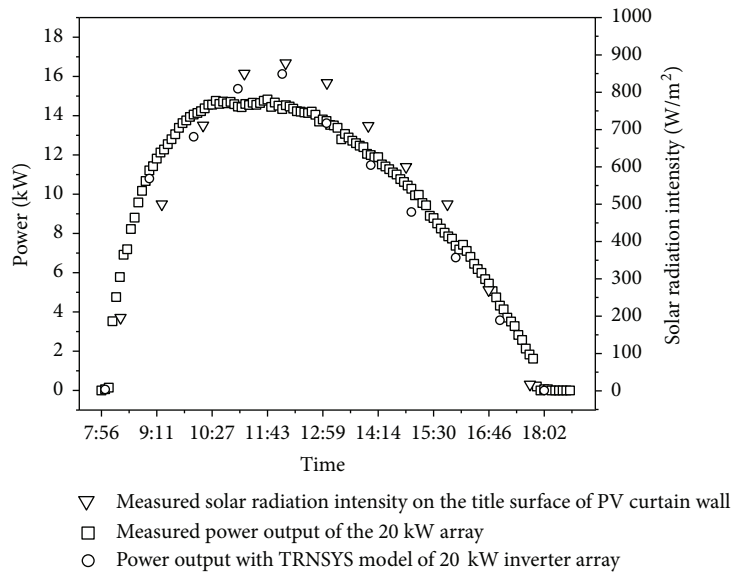


FIGURE 12: TRNSYS PV model validation for the power output of a day.

occurred in the year with the maximum recorded number of clear days [25]. So if there are no extreme weather events in a year, the PR of the BIPV system could be higher than 65%. While considering the typical degradation rate of PV modules (equal to 1%–2%/year) [24], the average value of PR could be 60% according to the simulated data of the TRNSYS model during the BIPV system with an expected lifetime of 25 years. The reason for the low PR of the BIPV system is that the area of solar cells in a module was just 48.5% of the total area of a PV module; however, the solar irradiation H in (1) includes all solar irradiation received by a module. In order to ensure partial light transmission and building daylighting, it is the only choice to sacrifice the efficiency of the PV module for the moment. From this view, it can be supposed that different types of solar cells and different designed schemes of the envelope curtain wall could improve the PR of a BIPV system; for example, a new kind of solar module which has a lower light transmittance,

known as a higher efficiency, would be employed to replace the existing one.

4.2. Environmental Assessment. It is generally known that the PV system is widely recognized as one of the most clean technologies for power generation. However, it consumes energy during its life cycle, particularly in the manufacturing processes, which may be larger than its energy output during its whole life. In order to thoroughly investigate the life cycle environmental effects and energy payback performance of the BIPV system, life cycle assessment (LCA) is used to measure its sustainability. LCA is usually used as a technique to compare and analyze various aspects associated with the development of a product and its potential impact throughout the product's life [28]. The goal of an LCA is to quantify nonrenewable (fossil) primary energy use and global warming potential in electricity generation. According to LCA, the life cycle primary energy use is considered the sum of

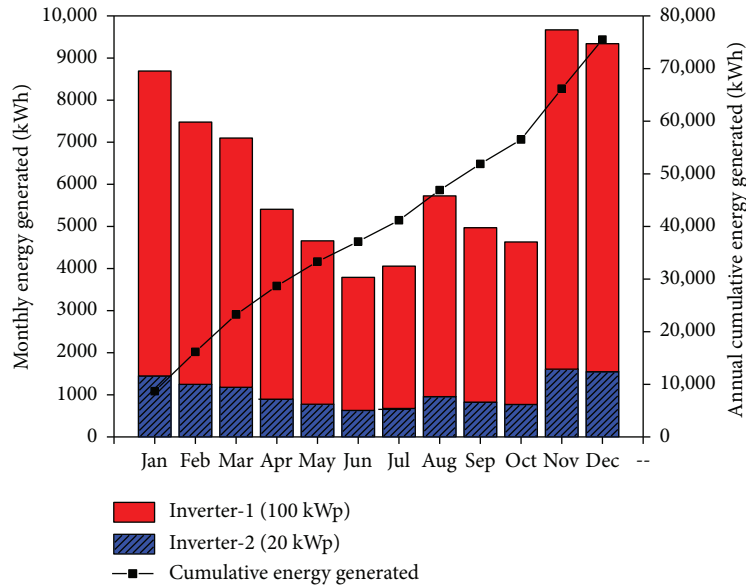


FIGURE 13: Predicted monthly BIPV power output using the TRNSYS model.

the energy consumed in three life cycle phases, which includes energy consumed in exploration, extraction, processing, manufacturing, decommissioning, and disposal of all the materials associated with the power generation system [29]. Besides, the energy payback time (EPBT) would be used, in order to find out whether the BIPV system can bring a net gain of energy for the user during its whole lifetime, and if so then to what extent. The EPBT is defined as the years required for a PV system to generate a certain amount of energy (converted into equivalent primary energy) for compensation of the energy consumption over its life cycle, including energy requirements in PV modules' manufacturing, assembly, transportation, system installation, operation and maintenance, and system decommissioning or recycling [30]. The equation of EPBT is presented as follows:

$$EPBT = \frac{E_{input} + E_{BOS,E}}{E_{output}}, \quad (2)$$

where E_{input} is the primary energy input of the PV module during the life cycle, which includes energy requirements in module manufacturing, transportation, installation, operation and maintenance, and module decommissioning or recycling [MWh]. $E_{BOS,E}$ is the energy requirement of the balance of system (BOS) components, which include support structures, cabling, electronic and electrical components, inverters, and batteries [MWh]. E_{output} is the annual primary energy savings due to electricity generation by the PV system [MWh].

There were very few papers using the actual energy yield to conduct an LCA study on BIPV systems in China, especially on a BIPV system of mono-Si modules, on account of many unavailable data of mono-Si production from the manufacturers, in particular, the energy consumption data of the Czochralski procedure. Besides,

different manufacturers have different energy requirements for silicon purification and crystallization processes, which increases the difficulty of the research. Lastly, there is a rapid technological improvement in the PV industry and cell production in China, and it is difficult to accurately estimate the energy requirements of mono-Si module production by experience. So this paper conducts the life cycle assessment study for the mono-Si BIPV system and discusses the energy payback performance just according to the data from literature [31–36].

The equivalent primary energy consumption for manufacturing solar mono-Si double-glazing PV modules is estimated as 4.67 MWh/kWp. And the BOS component is estimated as 1.12 MWh/kWp in this system, because the supporting structure is steel which is built outside the building exterior wall, and the battery can be saved in consideration of the special structure of the double-glazing module and the grid-connected scheme. And the energy consumption of the other components, including transportation, installation, operation and maintenance, and module decommissioning or recycling, would be 2-3 orders of magnitude lower than the energy consumption of PV module manufacturing and the BOS component; thus, they could be negligible when the life cycle energy requirement is calculated in the equation of EPBT. The EPBT of the BIPV system is calculated to be 9.38 years, so during the PV module's lifetime (normally expected to be 25 years), the BIPV system could still generate a substantial amount of electricity and gain additional benefits.

According to relevant Chinese documents of the National Bureau of Statistics, from the year 2006, the electricity consumption converted into the standard coal coefficient should employ the equivalent coefficient of 0.1229 kg/kWh, which means that 0.1229 kg of standard coal generates 1 kWh of power. The environmental benefits

TABLE 2: Environmental benefit measurement and relevant parameters for the BIPV system.

The major emission pollutants	Emission rate of pollutants (kg/kg _{ce})	Emission reduction density (kg/kWh)	Emission density (kg/kWh)	Environmental values of pollutants (RMB yuan/kg)	Environmental cost of generation (RMB yuan/kWh)	Environmental benefits of emission reduction (RMB yuan/kWh)
CO ₂	1.731	2.127×10^{-1}	7.986×10^{-2}	2.3×10^{-2}	0.184×10^{-3}	4.893×10^{-3}
SO ₂	0.018	2.212×10^{-3}	8.304×10^{-4}	6	4.983×10^{-3}	1.327×10^{-2}
NO _x	0.008	9.832×10^{-4}	3.691×10^{-4}	8	2.953×10^{-3}	7.866×10^{-3}
CO	0.00026	3.195×10^{-5}	1.199×10^{-5}	1	1.199×10^{-5}	3.195×10^{-5}
Particulate	0.11	1.351×10^{-2}	5.075×10^{-3}	1.2×10^{-1}	6.090×10^{-4}	1.622×10^{-3}
Slag	0.03	3.687×10^{-3}	1.384×10^{-3}	1.0×10^{-1}	1.384×10^{-4}	3.687×10^{-4}
Total	/	/	/	/	1.053×10^{-2}	2.805×10^{-2}

TABLE 3: The economic parameters [39].

Life span (years)	Annual output yield (MWh)	PV electricity tariff (RMB yuan/kWh)	Nominal interest rate	Inflation rate
25	75.515	0.6	4%	3%

of the BIPV system can be calculated as shown in Table 2, where the emission reduction density is calculated by the following formula [37]:

$$D_{er} = 0.1229 \times R_e, \quad (3)$$

where D_{er} is the emission reduction density while generating 1 kWh of power [kg/kWh] and R_e is the emission rate of pollutants per ton standard coal.

And the emission density is expressed using the following formula:

$$D_e = \frac{E_{c,l} \times D_{er}}{E_{g,l}}, \quad (4)$$

where D_e is the emission density [kg/kWh], $E_{c,l}$ is the total energy consumption of the BIPV system throughout the lifecycle [kWh], and $E_{g,l}$ is the total power generation of the entire life span [kWh]. The environmental cost of generation and the environmental benefits of emission reduction are calculated by the following, respectively:

$$\begin{aligned} C_g &= V_p \times D_e, \\ B_r &= R_e \times 0.1229 \times V_p, \end{aligned} \quad (5)$$

where C_g is the environmental cost of generating each kilowatt-hour of electricity [RMB/kWh], V_p is the environmental value of per ton of pollutants [RMB/kg], and B_r is the environmental benefit of emission reduction for each kilowatt-hour of electricity generated [RMB/kWh].

Because of the grid-connected BIPV system, the annual average emissions of CO₂, SO₂, NO_x, CO, particulates, and slag could be reduced by 1974 kg, 20.53 kg, 9.12 kg, 0.29 kg, 125.46 kg, and 34.22 kg, respectively. By calculation, as shown in Table 2, the environmental cost of the BIPV power generation system is RMB ¥0.01053 per kWh. Without the BIPV system, the environmental cost of power generation would be RMB ¥0.02805 per kWh through the thermal power, which means that the environmental cost could be

reduced by RMB ¥0.01752 per kWh due to the benefit of the BIPV system. Given that most parts of China have been affected by fog and haze, the environmental benefits should be a major consideration once such BIPV systems are widely applied in China.

4.3. Economic Analysis. This section shows the procedure followed to calculate the payback time for the BIPV system. The net present value (NPV) is used and can be expressed as follows [6, 38]:

$$NPV = \sum_{t=0}^p (CI - CO)(1 + i)^{-t}, \quad (6)$$

where CI is the cash inflows, CO is the cash outflows, i is the nominal interest rate, p is the life span of PV, in years, and t is the projected age limit. The higher the NPV, the better for the BIPV system, and when NPV is equal to 0, the payback period would be acquired. The initial cost of PV modules and the inverters in this system are RMB ¥20/Wp and RMB ¥1/Wp in the year of 2014, respectively. If including the supplying and fixing of steel framing, wires, and the data acquisition system, the total cost was equal to RMB ¥3,070,400. Fortunately, the public grant covered 80% of the total cost of the BIPV system, with an amount equal to RMB ¥2,500,000. The operation and maintenance (O&M) costs are approximately equal to 0.05%/year of the total cost. According to the real market prices and the expected electricity cost trend for the next years, the average commercial electric tariff for Kunming is expected to be RMB ¥0.6 (≈US \$0.1) per kWh; the annual average saving in electricity charge is computed to be RMB ¥45,309 (≈US \$7551.5). The other main economic parameters are shown in Table 3. On the basis of these considerations, the payback period is 15 years with government subsidy, and the NPV is RMB ¥359,347 at the end of a lifetime.

4.4. Energy Capacity Fraction of the Building. The building of the BIPV system in this study (Figure 1) is the Solar Energy

TABLE 4: The calculated results with different mounting tilt angles.

Tilt angles	90°	85°	80°	70°	60°
Annual power production (MWh)	68.685	75.515	82.359	95.617	107.311
EPBT (years)	10.32	9.38	8.60	7.41	6.60
Environmental cost of generation (RMB yuan/kWh)	1.158×10^{-2}	1.053×10^{-2}	0.965×10^{-2}	0.832×10^{-2}	0.741×10^{-2}
Payback period (years)	17	15	14	12	11
NPV (RMB yuan)	272,820	359,347	446,053	614,015	762,164

Research Institute in Yunnan Normal University; actually, much experimental equipment is placed in the building, including some high-power and high-energy-consuming facilities, for instance, the amorphous silicon thin-film solar cell production equipment, reheat furnaces, and wind tunnel testing facility. So it is meaningful to discuss the energy capacity fraction according to the Chinese national standard “Design standard for energy efficiency of public buildings” GB50189. Especially, because of the climate matter of Kunming, there is hardly any air-conditioning in the building. The lowest energy generation during the year is in June and July according to the results above; fortunately, this is the Chinese university summer vacation period, and so the energy consumption of the building is also the lowest. By the way, the previous research [40] found that due to the chimney effect of the PV curtain wall, the temperature of rooms covered by the PV curtain wall can keep warm without any heating facilities in winter; it can be regarded as another benefit of the BIPV to reduce the energy consumption of the building. Referring to the records of electricity consumption from 2014 up to now and comparing the annual energy consumption with annual cumulative power generation, it can be estimated that the average amount of energy consumed in the building is approximately 57,684 kWh each year in consideration of two long vacations and not any more new equipment, which is less than the amount produced from the photovoltaic system, which totaled 75,515 kWh. According to the definition of the capacity fraction (CF) in [41]

$$CF = \frac{E_{PV}}{E_{load}}, \quad (7)$$

where CF means the energy capacity fraction of the building, E_{PV} is the annual electricity produced by the PV array, and E_{load} is the annual electricity consumed by the load. Therefore, the final energy capacity fraction is 130.91%, and the energy surplus is 17,831 kWh, which means that the goal of the zero-energy building is achieved. However, few facilities have not been put into full operation in the building, and obviously, the total energy consumption of the building could not be covered by the PV system at all in the future, while taking into account so many experimental facilities fully running. In order to improve the energy capacity fraction, it is possible to optimize the PV panel tilt angle or reduce the operating temperature in order to maximize the electricity production.

5. Discussion

As discussed above, it can be found that the energy payback time (EPBT), the environmental cost, the NPV, and so on, as well as all the performance parameters of the BIPV system are closely related to the amount of power generation. The higher the power generation, the more advantages the BIPV system has, and the main influencing factors to power generation are the solar radiation intensity and the efficiency of the PV modules. The efficiency of the semitransparent PV modules could not be as high as that of the traditional PV modules with opaque panels, since partial light transmission and building daylighting must be ensured, leading to certain areas in a module that have to be sacrificed. However, with the technologies developing, maybe the efficiency of the semitransparent PV modules used in a BIPV system would be improved significantly in the future. At present, the simple and efficient method to increase the power generation is to change the mounting tilt angles of the PV curtain wall. The yearly PV power generations have been calculated with different tilt angles by the TRNSYS models; the results are shown in Table 4.

With the mounting tilt angle decreasing from 90° to 60°, the annual power production increases from 68.685 MWh to 107.311 MWh gradually, because the PV modules could receive more solar radiation at the 60° tilt angle than at 90° for a full year. Though more power production can be achieved with a smaller tilt angle, it is impossible for a BIPV system, especially the PV curtain wall integrated with a building, to design a tilt angle smaller than 60 degrees, except in a rooftop PV system. The EPBT, environmental cost of generation, and payback period would reduce with the decrease in tilt angles, and it is beneficial for a designer to decide which angle would be chosen, according to different emphasis points. The payback period and the NPV also are affected by other important factors, such as the total cost of the BIPV system, the nominal rate of interest, and the rate of inflation. In this work, a lot of state subsidies are provided; thus, the payback period can be shortened and benefits can be gotten in its life span. If the nominal interest rate and the inflation rate change in the next 30 years and the government subsidy still remains to be RMB ¥2,500,000, the payback period would be extended. Moreover, the amount of government subsidies plays an essential part in the payback period and NPV of this kind of BIPV systems. The effect of different interest rates and the amount of government subsidy on the payback period and NPV is calculated in Table 5. If the government subsidy reduces to less than

TABLE 5: The variation of the payback period and NPV with the interest rate.

Government subsidy (RMB yuan)	2,500,000	2,500,000	2,500,000	2,200,000	2,400,000	2,600,000
Nominal interest rate	4.00%	4.50%	4.25%	4.00%	4.00%	4.00%
Inflation rate	3.00%	2.00%	1.50%	3.00%	3.00%	3.00%
Real rate of interest [39]	0.97%	2.45%	2.71%	0.97%	0.97%	0.97%
Payback period (years)	15	17	18	24	18	13
NPV (RMB yuan)	359,347	211,565	189,551	62,133	260,210	458,287

RMB ¥2,150,000, the cost of investment could not be recovered during the 25-year life span. Nevertheless, the environmental effects should be beyond the economic benefits; more and more, the similar BIPV system would be employed with the decrease in PV costs. And all of the results above show the comprehensive analysis procedure of a BIPV system, including the methods of evaluation and prediction, which can be referenced for system designing.

6. Conclusions

A study of the operational performance of a grid-connected building-integrated photovoltaic (BIPV) system, a 120 kWp monocrystalline, in Kunming, China, was conducted. The experimental results from October 2014 to September 2015 have been analyzed and have been compared with a TRNSYS model, which provides good agreement with the experimental results. Moreover, the TRNSYS model has been built to predict the amount of power generation of the BIPV system under the meteorological database of Meteororm, and the annual electricity production of 75.515 MWh was estimated.

The PR of the BIPV system was calculated with the test data of the first year of installation (the year 2015), which was equal to 64.3%. However, according to the simulated data of the TRNSYS model during the BIPV system expecting a lifetime of 25 years, the average value of PR could be 60%. Based on the PR and LCA of the system, the EPBT is calculated to be 9.38 years, which shows that the BIPV system could still generate a substantial amount of electricity in its expected lifetime. Besides, the annual average emissions of CO₂, SO₂, NO_x, CO, particulates, and slag could be reduced by 1974 kg, 20.53 kg, 9.12 kg, 0.29 kg, 125.46 kg, and 34.22 kg, respectively, after the adoption of the BIPV power generation system, the environmental cost of which is RMB ¥0.01053 per kWh and with the environmental economic benefit of RMB ¥0.01752 per kWh. Consequently, the net present value (NPV) and the economic payback time of the BIPV system were estimated. The NPV is equal to approximately RMB ¥359,347 at the end of the life span, and the payback is 15 years. These results mean that the system has both good environmental and economic benefits. Not only that, the BIPV system is also effective in helping the building to achieve the zone energy consumption goal; in other words, nearly all of the existing building's energy consumption could be covered by the power generation of the installed BIPV system so far, even a surplus. The results can be used as the reference for future studies related to

improving the performance of the BIPV system or be effectively extended to the investigation of other BIPV systems.

Conflicts of Interest

The authors declare that they have no conflicts of interest.

Acknowledgments

This work is supported by a grant from the Yunnan Province Science Foundation for Youths (2014FD015).

References

- [1] *IEA World Energy Outlook 2013*, International Energy Agency, 2013.
- [2] L. Pérez-Lombard, J. Ortiz, and C. Pout, "A review on buildings energy consumption information," *Energy and Buildings*, vol. 40, no. 3, pp. 394–398, 2008.
- [3] X. Kong, S. Lu, P. Gao, N. Zhu, W. Wu, and X. Cao, "Research on the energy performance and indoor environment quality of typical public buildings in the tropical areas of China," *Energy and Buildings*, vol. 48, pp. 155–167, 2012.
- [4] S. Kadoshin, T. Nishiyama, and T. Ito, "The trend in current and near future energy consumption from a statistical perspective," *Applied Energy*, vol. 67, no. 4, pp. 407–417, 2000.
- [5] M. J. Ritzen, Z. A. E. P. Vroon, R. Rovers, and C. P. W. Geurts, "Comparative performance assessment of a non-ventilated and ventilated BIPV rooftop configurations in the Netherlands," *Solar Energy*, vol. 146, pp. 389–400, 2017.
- [6] W. Wang, Y. Liu, X. Wu et al., "Environmental assessments and economic performance of BAPV and BIPV systems in Shanghai," *Energy and Buildings*, vol. 130, pp. 98–106, 2016.
- [7] L. Y. Seng, G. Lalchand, and G. M. Sow Lin, "Economical, environmental and technical analysis of building integrated photovoltaic systems in Malaysia," *Energy Policy*, vol. 36, no. 6, pp. 2130–2142, 2008.
- [8] L. Aelenei, R. Pereira, A. Ferreira, H. Gonçalves, and A. Joyce, "Building integrated photovoltaic system with integral thermal storage: a case study," *Energy Procedia*, vol. 58, pp. 172–178, 2014.
- [9] A. G. Hestnes, "Building integration of solar energy systems," *Solar Energy*, vol. 67, no. 4–6, pp. 181–187, 1999.
- [10] G. C. Bakos and M. Soursos, "Technical feasibility and economic viability of a grid-connected PV installation for low cost electricity production," *Energy and Buildings*, vol. 34, no. 7, pp. 753–758, 2002.
- [11] B. Norton, P. C. Eames, T. K. Mallick et al., "Enhancing the performance of building integrated photovoltaics," *Solar Energy*, vol. 85, no. 8, pp. 1629–1664, 2011.

- [12] D. H. W. Li, T. N. T. Lam, W. W. H. Chan, and A. H. L. Mak, "Energy and cost analysis of semi-transparent photovoltaic in office buildings," *Applied Energy*, vol. 86, no. 5, pp. 722–729, 2009.
- [13] D. H. W. Li, S. K. H. Chow, and E. W. M. Lee, "An analysis of a medium size grid-connected building integrated photovoltaic (BIPV) system using measured data," *Energy and Buildings*, vol. 60, pp. 383–387, 2013.
- [14] T. Hong, C. Koo, J. Park, and H. S. Park, "A GIS (geographic information system)-based optimization model for estimating the electricity generation of the rooftop PV (photovoltaic) system," *Energy*, vol. 65, pp. 190–199, 2014.
- [15] B. Celik, E. Karatepe, S. Silvestre, N. Gokmen, and A. Chouder, "Analysis of spatial fixed PV arrays configurations to maximize energy harvesting in BIPV applications," *Renewable Energy*, vol. 75, pp. 534–540, 2015.
- [16] F. Cucchiella and I. D'Adamo, "Estimation of the energetic and environmental impacts of a roof-mounted building-integrated photovoltaic systems," *Renewable and Sustainable Energy Reviews*, vol. 16, no. 7, pp. 5245–5259, 2012.
- [17] H. Radhi, "Energy analysis of façade-integrated photovoltaic systems applied to UAE commercial buildings," *Solar Energy*, vol. 84, no. 12, pp. 2009–2021, 2010.
- [18] R. Eke and A. Senturk, "Monitoring the performance of single and triple junction amorphous silicon modules in two building integrated photovoltaic (BIPV) installations," *Applied Energy*, vol. 109, pp. 154–162, 2013.
- [19] S. Wittkopf, S. Valliappan, L. Liu, K. S. Ang, and S. C. J. Cheng, "Analytical performance monitoring of a 142.5kW_p grid-connected rooftop BIPV system in Singapore," *Renewable Energy*, vol. 47, pp. 9–20, 2012.
- [20] S. Kang, T. Hwang, and J. T. Kim, "Theoretical analysis of the blinds integrated photovoltaic modules," *Energy and Buildings*, vol. 46, pp. 86–91, 2012.
- [21] S. Li, J. Joe, J. Hu, and P. Karava, "System identification and model-predictive control of office buildings with integrated photovoltaic-thermal collectors, radiant floor heating and active thermal storage," *Solar Energy*, vol. 113, pp. 139–157, 2015.
- [22] *Solar Energy Laboratory User Manual: TRNSYS 17 a TRAn-sient SYstem Simulation Program – Volume 4 – Mathematical Reference*, vol. 4, 2009.
- [23] B. Quesada, C. Sánchez, J. Cañada, R. Royo, and J. Payá, "Experimental results and simulation with TRNSYS of a 7.2 kWp grid-connected photovoltaic system," *Applied Energy*, vol. 88, no. 5, pp. 1772–1783, 2011.
- [24] M. Kumar and A. Kumar, "Performance assessment and degradation analysis of solar photovoltaic technologies: a review," *Renewable and Sustainable Energy Reviews*, vol. 78, pp. 554–587, 2017.
- [25] N. Aste, C. Del Pero, and F. Leonforte, "The first Italian BIPV project: case study and long-term performance analysis," *Solar Energy*, vol. 134, pp. 340–352, 2016.
- [26] S. Li Causi, S. Castello, and F. De Lia, "ENEA role in the Italian roof-top programme," in *Proceedings of 3rd World Conference on Photovoltaic Energy Conversion, 2003*, vol. 3, pp. 2644–2647, Osaka, Japan, May 2003.
- [27] N. Aste, C. Del Pero, and F. Leonforte, "PV technologies performance comparison in temperate climates," *Solar Energy*, vol. 109, pp. 1–10, 2014.
- [28] A. F. Sherwani and J. A. Usmani, "Life cycle assessment of solar PV based electricity generation systems: a review," *Renewable and Sustainable Energy Reviews*, vol. 14, no. 1, pp. 540–544, 2010.
- [29] R. Kannan, K. C. Leong, R. Osman, and H. K. Ho, "Life cycle energy, emissions and cost inventory of power generation technologies in Singapore," *Renewable and Sustainable Energy Reviews*, vol. 11, no. 4, pp. 702–715, 2007.
- [30] J. Peng, L. Lu, and H. Yang, "Review on life cycle assessment of energy payback and greenhouse gas emission of solar photovoltaic systems," *Renewable and Sustainable Energy Reviews*, vol. 19, pp. 255–274, 2013.
- [31] M. J. (Mariska) de Wild-Scholten, "Energy payback time and carbon footprint of commercial photovoltaic systems," *Solar Energy Materials & Solar Cells*, vol. 119, pp. 296–305, 2013.
- [32] Y. Jia, J. Wang, Z. Han, Y. Pang, and P. An, "Analysis on environmental load of wind, PV and coal-fired power generation based on life cycle assessment," *Journal of Chinese Society of Power Engineering*, vol. 36, pp. 1000–1009, 2016.
- [33] L. Pei, *The study on eco-design of high-rise residential buildings in Wuhan based on energy simulation and life cycle assessment*, Huazhong University of Science and Technology, Wuhan, China, 2015.
- [34] Y. Li, *Life cycle assessment of crystalline silicon modules in China*, Shanghai Jiao Tong University, Shanghai, China, 2015.
- [35] J. X. Zhang and G. F. Zhu, "Comparative studies of photovoltaic power generation and coal-fired power generation base on life cycle assessment," *Environmental Science and Management*, vol. 39, pp. 86–90, 2014.
- [36] Y. He, J. Zhang, Q. Wang, and J. Xie, "Environmental impact assessment on multicrystalline wafer production based on life cycle assessment method," *Sichuan Environment*, vol. 32, pp. 83–90, 2013.
- [37] Y. Sun, R. Wang, L. Xiao, J. Liu, Y. Yu, and X. Zhuang, "Economical and environmental analysis of grid-connected photovoltaic system in China," *China Population, Resources and Environment*, vol. 21, pp. 88–94, 2011.
- [38] Q. Zhu, L. Si, and T. Jiang, "Economical and environmental analysis of building photovoltaic systems with different installation styles," *Acta Energetica Solaris Sinica*, vol. 33, pp. 24–29, 2012.
- [39] G. Evola and G. Margani, "Renovation of apartment blocks with BIPV: energy and economic evaluation in temperate climate," *Energy and Buildings*, vol. 130, pp. 794–810, 2016.
- [40] Y. F. Wang, R. H. E. Hassanien, M. Li, G. X. Xu, and X. Ji, "An experimental study of building thermal environment in building integrated photovoltaic (BIPV) installation," *Bulgarian Chemical Communications*, vol. 48, pp. 158–164, 2016.
- [41] A. Gallo, B. T. Molina, M. Prodanovic, J. G. Aguilar, and M. Romero, "Analysis of net zero-energy building in Spain. Integration of PV, solar domestic hot water and air-conditioning systems," *Energy Procedia*, vol. 48, pp. 828–836, 2014.

